Int J Clin Exp Med 2015;8(6):8506-8515
www.ijcem.com /ISSN:1940-5901/IJCEM0007780

Original Article

Ultrasound elastography and magnetic resonance examinations are effective for the accurate diagnosis of mammary duct ectasia

Feixue Zhang[1], Dexin Yu[2], Mingming Guo[3], Qing Wang[2], Zhigang Yu[3], Fei Zhou[3], Meng Zhao[2], Feng Xue[2], Guangrui Shao[4]

[1]Department of Radiology, Division of Ultrasound, The Second Hospital of Shandong University, Jinan City, Shandong Province, P.R. China; [2]Department of Radiology, Qilu Hospital, Shandong University, Jinan City, Shandong Province, P.R. China; [3]Department of Breast Surgery, The Second Hospital of Shandong University, Jinan City, Shandong Province, P.R. China; [4]Department of Radiology, The Second Hospital of Shandong University, Jinan City, Shandong Province, P.R. China

Received March 10, 2015; Accepted May 28, 2015; Epub June 15, 2015; Published June 30, 2015

Abstract: Objectives: This study is to investigate the values of multiple quantitative evaluation parameters in the diagnosis of mammary duct ectasia (MDE), using real-time ultrasound elastography (UE) and magnetic resonance imaging (MRI). Methods: This retrospective study was performed on 15 patients (16 lesions) with MDE. Ultrasound examination was performed with the LOGIQ E9 ultrasound instrument, with all lesions being examined by routine ultrasound and UE. MRI examination was performed with a Signa HD × 3.0T TWINSP MR System, including of plain-scan, diffusion-weighted imaging, dynamic contrast-enhanced MRI, and proton magnetic resonance spectroscopy. Imaging features, as well as semi-quantitative and quantitative parameters, were analyzed to determine their diagnostic value for MDE. Results: According to the five-point scale in UE, twelve lesions belonged to 1-3 point scale, and four lesions were in 4-5 point scale, with an average of 2.93 ± 0.77. In dynamic contrast-enhanced MRI, the lesions appeared as obviously enhanced signals. The MRI early-enhancement rate ranged from 0.35 to 1.07 (0.67 ± 0.30 on average); the time peak ranged between 192 and 330 s (248 ± 37 s on average); the peak-enhancement ratio ranged from 2.26 to 3.06, with an average of 2.59 ± 0.33. According to MRI time-signal intensity curves classified into persistently enhancing (type I), plateau (type II) and washout (type III), 12 lesions (75%) belonged to type I, three (18.75%) belonged to type II, and one (6.25%) belonged to type III. Magnetic resonance spectroscopy showed that a total choline peak occurred only in one lesion. The diagnosis accuracy rates for ultrasound alone, MRI alone and the combination of ultrasound and MRI were 75% (12/16), 87.5% (14/16) and 93.75% (15/16), respectively. Conclusions: Both ultrasound and MRI show clinical importance in MDE diagnosis. However, UE, dynamic contrast-enhanced MRI, and magnetic resonance spectroscopy demonstrate significantly better diagnosis and differential diagnosis of MDE.

Keywords: Mammary duct ectasia, ultrasound, magnetic resonance imaging, magnetic resonance spectroscopy, ultrasound elastography

Introduction

Mammary duct ectasia (MDE) is a type of non-puerperal benign mastitis with an incidence of 1.1-75% depending on the diagnostic methods used [1]. Historically, MDE descriptions involved diverse terminologies, according to different histological and symptomatic features [2]. However, Haagensen et al. proposed using MDE as the formal and unified name in 1951, based on its major pathological feature - a blocked or clogged lactiferous duct [3]. The diagnosis of MDE is clinically challenging because of its diversified and complex symptoms [2] as well as its resemblance to breast cancer in some cases [4]. Inappropriate diagnosis or treatment can result in recurrent onset and persistent symptoms. For example, misdiagnosis of breast cancer can lead to complete breast resection [5]. Accurate and timely differential diagnoses are critical for the treatment of MDE.

Imaging examinations that can identify mammary diseases include mammography, ultrasound (US), magnetic resonance imaging (MRI)

and galactography [6]. Each method has its unique advantages and disadvantages. For instance, mammography provides superior sensitivity to calcification [6] and is optimal for the diagnosis of dense breast tissue, but its specificity is relatively low [7]. Galactography is sensitive to minor intraductal lesions, but it can be unsuccessful if the pathologic ducts cannot be cannulated [8]. In addition, some patients may feel uncomfortable during galactography [6]. In general, most MDE can be diagnosed by routine US [9], which typically shows thickened walls of mammary ducts with widening lumen (> 3 mm) or fistulae connected with abscesses [9]. The diagnosis of large lesions can be difficult and differential diagnosis is often required in the presence of inflammation for breast cancer [10, 11]. Although real-time ultrasound elastography (UE) can provide informative images that distinguish between benign and malignant lesions [12, 13], there are few reports on its use for MDE diagnosis. For soft tissues, high-resolution MRI proves advantageous for the diagnosis of mammary diseases [14, 15]. However, its ability to differentiate between benign and malignant mastitis remains controversial [11, 14, 16, 17]. Quantitative measurements could significantly reduce subjective evaluation required for images obtained from ultrasound or MRI, and improve diagnosis accuracy. This study used UE and MRI to investigate the diagnostic value of quantitative measurements in clinical treatment of MDE patients.

Materials and methods

Patients

A total of 15 MDE patients were recruited for studying a total of 16 lesions between May 2012 and June 2013. They were first examined by routine US, which could not make definitive diagnosis. Afterwards, the patients were examined by UE and MRI, followed by mammotome biopsy within seven days after the imaging examination, before the samples were sent for pathological investigations. All examinations were carried out within a week. The diagnosis of MDE complicated with/without acute and chronic inflammation, abscess, or granuloma was made after excluding inflammatory breast carcinoma, other infective and non-infective causes of inflammation (such as tuberculosis, parasitic and fungal infections, and sarcoidosis), Wegener's granulomatosis, giant cell arteritis, polyarteritis nodosum, idiopathic granulomatous mastitis and lactational mastitis [18]. All patients were female with ages between 24 and 48 years (average 34 ± 7.12 years). Among the 15 patients, 14 patients were married with histories of childbearing (one childbirth for 10 patients and two childbirths for the other 4 patients). Ten patients had a history of bilateral breastfeeding with only two having galactostasia, two patients had a history of single-breast breastfeeding without galactostasia, one patients had a history of single-breast breastfeeding with galactostasia and one patient had no breastfeeding but had galactostasia. One patient had never been married or given birth to babies. For all patients, MDE onset occurred over a period ranging between four days and half a year. Local masses and tenderness in the breast, as major clinical manifestations, occurred in 10 patients; local masses without tenderness occurred in 3 patients; and tenderness without masses occurred in 2 patients. Four patients suffered from skin irritation, and 3 showed skin ulceration with sinus formation. Five patients had nipple inversion (bilateral in one patient) and three patients experienced nipple discharge (white liquid in two patients and purulent liquid in one). All 15 patients had normal menstruation, no history of smoking, no history of hepatitis, diabetes, or tuberculosis and no family history of breast cancer. The study was approved by the Medical Ethics Board of The Second Hospital of Shandong University. Informed consent was obtained from all patients or their families.

US

US examination was performed with the LOGIQ E9 ultrasound instrument (GE Healthcare, Little Chalfont, UK). The breasts of each patient were fully exposed in a supine position with the arms being raised above the head. A 9-14 MHz high-frequency probe was used to scan the breasts and axillaries of the patients bilaterally. UE was performed after routine US. Routine US and UE were performed by two specified senior experts, each with at least 5 years of experience in breast US.

According to the routine US features [19], all lesions were classified into four types: mammary-duct dilation (type I), cyst-and-solid mass

Table 1. The diagnostic results of ultrasound, magnetic resonance imaging and the combination of both

	US	MRI	US + MRI	Pathology
MDE	12	14	15	16
IDP	1	0	0	0
IBC	2	2	1	0
IPC	1	1	0	0

Note: US, ultrasound; MRI, magnetic resonance imaging; MDE, mammary duct ectasia; IDP: intraductal papilloma; IBC, inflammatory breast cancer; IPC, intraductal papillary carcinoma.

(type II), solid mass (type III), and abscess (type IV). A five-point scale was adopted according to the hardness of nodules, as seen in UE [20, 21]: a lesion that showed green overall (or mostly) scored 1 point; if the center of a lesion appeared to be blue and surrounded by dominant green, it scored 2 points; a lesion exhibiting equal amount of green and blue colors scored 3 points; a lesion appearing predominately blue, or blue mixed with a little green, scored 4 points; if the surrounding tissues of a lesion appeared to be blue, with or without green inside, the lesion scored 5 points. A lesion scoring from 1 to 3 points was considered benign, while that scoring 4 or 5 points was malignant.

The classification and scoring were performed by the same two specified experts. Two-dimensional images, color Doppler flow imaging (CDFI) and elastography were recorded and archived. All data was analyzed by the two specified senior experts according to Breast Imaging-Reporting and Data System (BI-RADS) lexicon of the American College of Radiology (ACR) [22]. If the experts did not agree with each other, they would ask for a superior.

MRI

MRI examination was performed with a Signa HD × 3.0T TWINSP MR System (GE Healthcare, Little Chalfont, UK) with a special coil made for breast examination (bilateral eight channel coil). With the patient being in a prone position, the breasts were placed on, and suspended by the examination coil. MRI plain scanning was performed from the direction of the feet using the parameters of Ax STIR (TR 8200/TE 36, Matrix 512 × 512, NEX 2.00), Ax T1FSE (TR 40/TE 7.9, NEX 2.00, Matrix 512 × 512) and bilateral sag (TR3600/TE110, Matrix 512 × 512, NEX 2.00), and diffusion-weighted imaging (b = 0, 1000) (TR6000/TE70, Matrix 512 × 512, NEX 4.00). Dynamic contrast-enhanced (DCE)-MRI scanning was conducted by injecting the contrast medium Gadolinium (Gd)-diethylene triamine pentacetate acid at a dosage of 0.2 mmol/kg in 20 ml saline into dorsum manus vein at a speed of 1.5 ml/s, followed by another 20 ml saline. A scanning mask was obtained before contrast medium injection, and 3-dimensional vibrant-axial scanning was carried out at the same time with the injection of the contrast medium (parameters: TR 4.3/TE 2.1, Matrix 512 × 512, NEX 0.7) for eight phases. Then, 3-dimensional vibrant-sagittal scanning was performed (parameters: TR 4.3/TE 1.8, Matrix 512 × 512, NEX 0.7). Proton (^{1}H) magnetic resonance spectroscopy (MRS) was conducted with a minimum volume of interest of 15 × 15 × 15 mm (parameters: TR2000/TE155, NEX32, FOV36), which avoided areas of necrosis and cysts.

All data were processed off-line on an AW Volume share 2 workstation, and independently interpreted by two senior experts, each with at least 10 years of experience in MRI diagnosis. Radiologists were blinded to the final pathological results. The morphological features of the lesions were analyzed according to Breast Imaging-Reporting and Data System (BI-RADS) lexicon of the American College of Radiology (ACR) [22]. The measurement parameters included early-stage enhancement ratio (EER), peak-of-enhancement ratio (PER), time peak (Tpeak) and time-signal intensity curve. The formula for EER calculation is: $EER = S_1 - S_0/S_0 \times 100\%$, in which S_1 is the signal intensity obtained 1 minute after contrast medium injection and S_0 is the signal intensity obtained before injection. The formula for calculating PER is: $PER = S_{peak} - S_0/S_0 \times 100\%$, in which S_{peak} is the peak signal intensity obtained before or after contrast medium injection and S_0 is the signal intensity obtained before injection. Tpeak is the time between contrast medium injection and the highest signal intensity. Time-signal intensity curve (TIC) was classified into three types [23]: persistently enhancing (type I), plateau (type II) and washout (type III).

Statistical analysis

All data were analyzed using SPSS 17.0 for Windows (IBM, USA). Measurement materials were expressed as means ± standard devia-

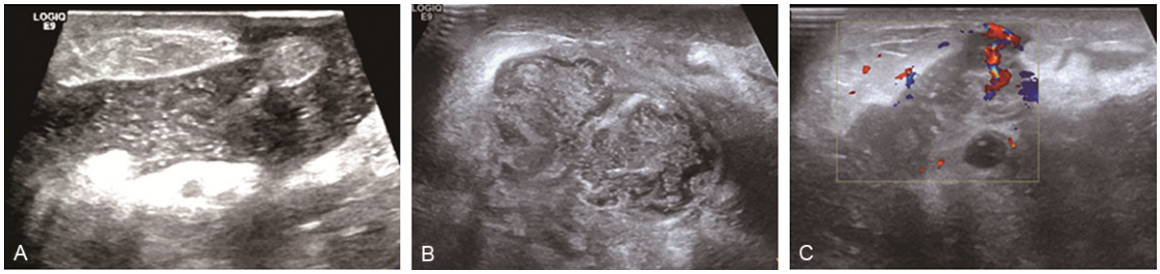

Figure 1. US of a 28 year-old female with MDE complicated with inflammation and abscess. (A) The dilated mammary duct was beneath and to the lateral of the nipple. There were fine spots within the duct, flowing upon squeezing. The skin was involved with ulceration. (B) The lesion was large with disordered morphology. A localized liquid dark area was visible, with weak signal and flowing fine spots. (C) CDFI indicated moderate blood flow within the lesion.

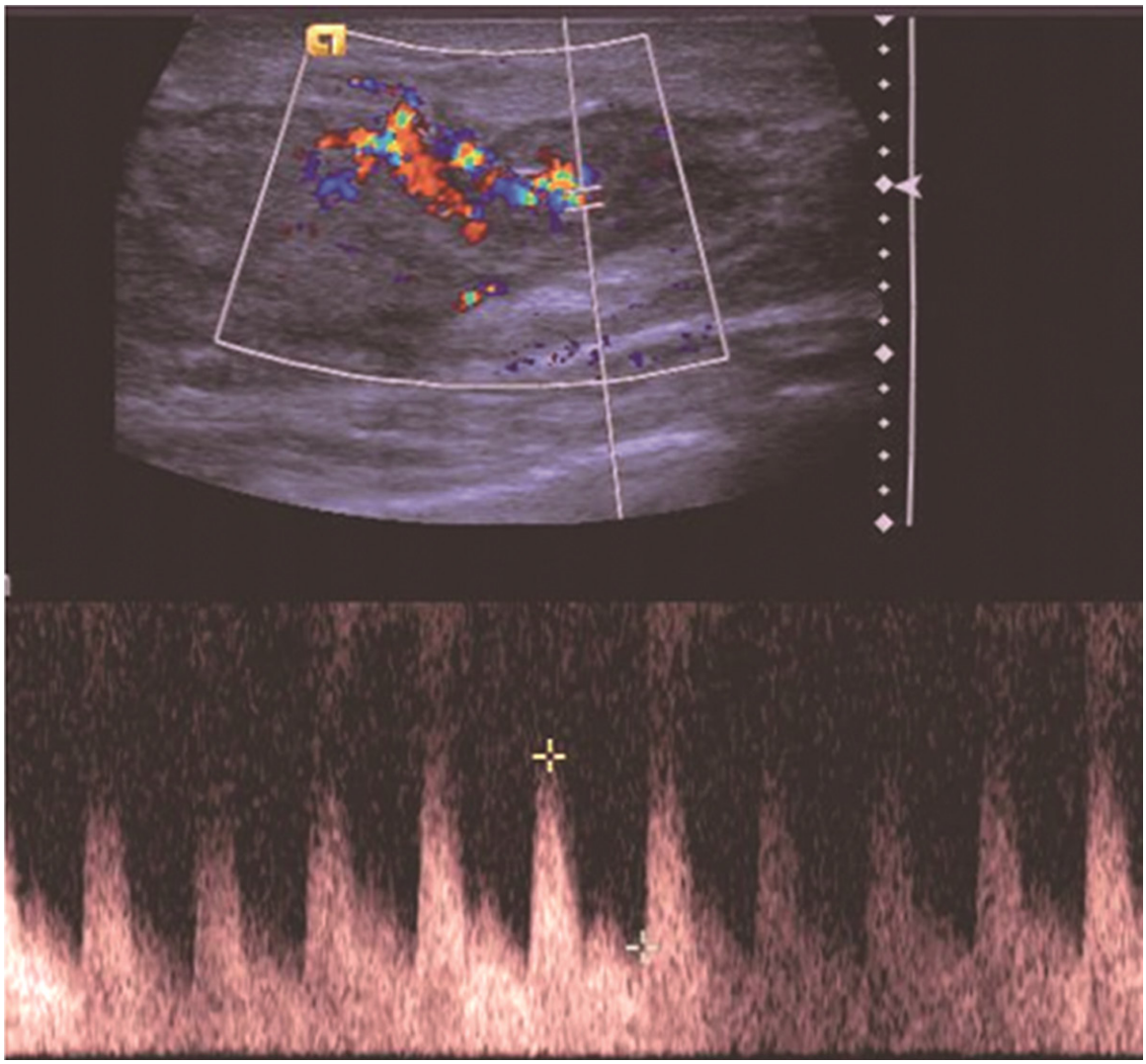

Figure 2. Color Doppler flow imaging (CDFI) of a 48 year-old female with MDE. CDFI indicated abundant blood flow with at least four visible vessels of varied diameter in the view. The RI value was 0.61.

tions. The difference of diagnostic accuracies among US, MRI and the combination of US and MRI were compared by Chi-square test. Paired comparisons of US, MRI and the combination of

Table 2. Relationship between types and elastography scores

	1	2	3	4	5	Total
Type I	0	1	0	0	0	1
Type II	0	2	2	2	0	6
Type III	0	1	1	1	0	3
Type IV	0	1	4	1	0	6
Total	0	5	7	4	0	16

US and MRI were performed using Fisher's exact test. $P < 0.05$ indicates significant difference.

Results

US

To determine the diagnostic results of US, we combined routine US with UE. The diagnostic results are shown in **Table 1**. All 16 lesions were classified into four types based on MDE features: type I, one lesion (6.25%); type II, six lesions (37.5%); type III, three lesions (18.75%); and type IV, six lesions (37.5%) (**Figure 1A-C**). Furthermore, the resistance index (RI) ranged between 0.52 and 0.66 (0.593 ± 0.042 on average) (**Figure 2**). Elastography results (**Table 2**) showed an average score of 2.93 ± 0.77 (**Figure 3A**, **3B**). These data suggest that routine US is able to show the morphological features while RI and UE can identify malignant tumors.

MRI

To investigate the accuracy of MRI examination, MRI plain-scan was used. The diagnostic results are shown in **Table 1**. Typical accompanying signs included mammary gland or chest wall edema in five lesions, inverted nipples in six lesions, thickened or sunken skin in four lesions, sinus formation in four lesions, thickened vascular wall in eight lesions and enlarged lymph nodes in eight lesions (**Table 3**). The apparent diffusion coefficient (ADC) of the lesions ranged between 1.01 and 2.30 × 10^{-3} mm^2/s (1.31 × 10^{-3} ± 0.19 mm^2/s on average). DCE-MRI indicated that the 16 lesions exhibited a significantly enhanced signal (**Figure 4A**, **4B**). A ring-like enhancement with a thickened wall was found in six lesions (**Figure 5A-D**); patchy or nodular enhancement was found in six lesions; and irregular enhancement was found in four lesions (**Table 3**). All lesions showed clear boundaries with surrounding tissues although the edges were not smooth. Detailed measurements indicated an EER ranging between 0.35 and 1.07 (0.67 ± 0.30 on average), a Tpeak ranging between 192 and 330 s (248 ± 37 s on average) and PER ranging between 2.26 and 3.06 (2.59 ± 0.33 on average). The time-signal intensity curve (TIC) of all 16 lesions were classified into three types: 12 lesions (75%) in type I (**Figure 6A**), 3 lesions (18.75%) in type II (**Figure 6B**) and 1 lesion (6.25%) in type III (**Figure 6C**). The total Choline peak (tCho) was only found in one lesion (**Figure 7A**, **7B**). These data indicate that semi-quantitative and quantitative parameters of MRI are helpful for the diagnosis of MDE.

The combination of US and MRI

To further investigate the effect of US and MRI, we combined US and MRI. The diagnostic results are shown in **Table 1**. UE ruled out 1 case of inflammatory breast cancer diagnosed by MRI. Using TIC, MRI ruled out 1 case of intraductal papilloma, 1 lesion of intraductal carcinoma and 1 case of inflammatory breast cancer diagnosed by US. Only 1 case of inflammatory breast cancer was diagnosed by the combination of US and MRI. These data suggest that higher accuracy can be acquired by analyzing more parameters using the combination of US and MRI.

Pathological examinations and follow-ups

To evaluate the accuracy of US, MRI and their combination, samples were sent for pathological examinations afterwards. The pathological results were gold standard. The data showed that 16 lesions were MDE with/without inflammation, abscess, or granuloma (**Table 1**). There were no significant differences among the diagnosis accuracy rates for US, MRI and their combination (**Table 4**). One out of the 15 patients failed to provide follow-up data, 3 patients who underwent partial resection showed no recurrence till the end of the follow-up period, and 11 patients underwent treatment with isoniazid (0.3 g/d), rifampicin (0.45 g/d), and ethambutol (0.75 g/d). Two patients in this group stopped medication and showed no recurrence; another 9 patients under treatments showed lesion shrink, although 3 out of the 9 patients suffered from local ulcerations when

Table 3. Features of MRI plain-scan images

	Signal						Morphology		Boundary	
	High	Equal	Low	Mixed	Homogeneous	Heterogeneous	Regular	Irregular	Clear	Unclear
STIR	10		2	4	4	12	4	12	6	10
T1FSE	4	2	8	2	6	10	4	12	8	8
DWI	16					16	4	12	6	10

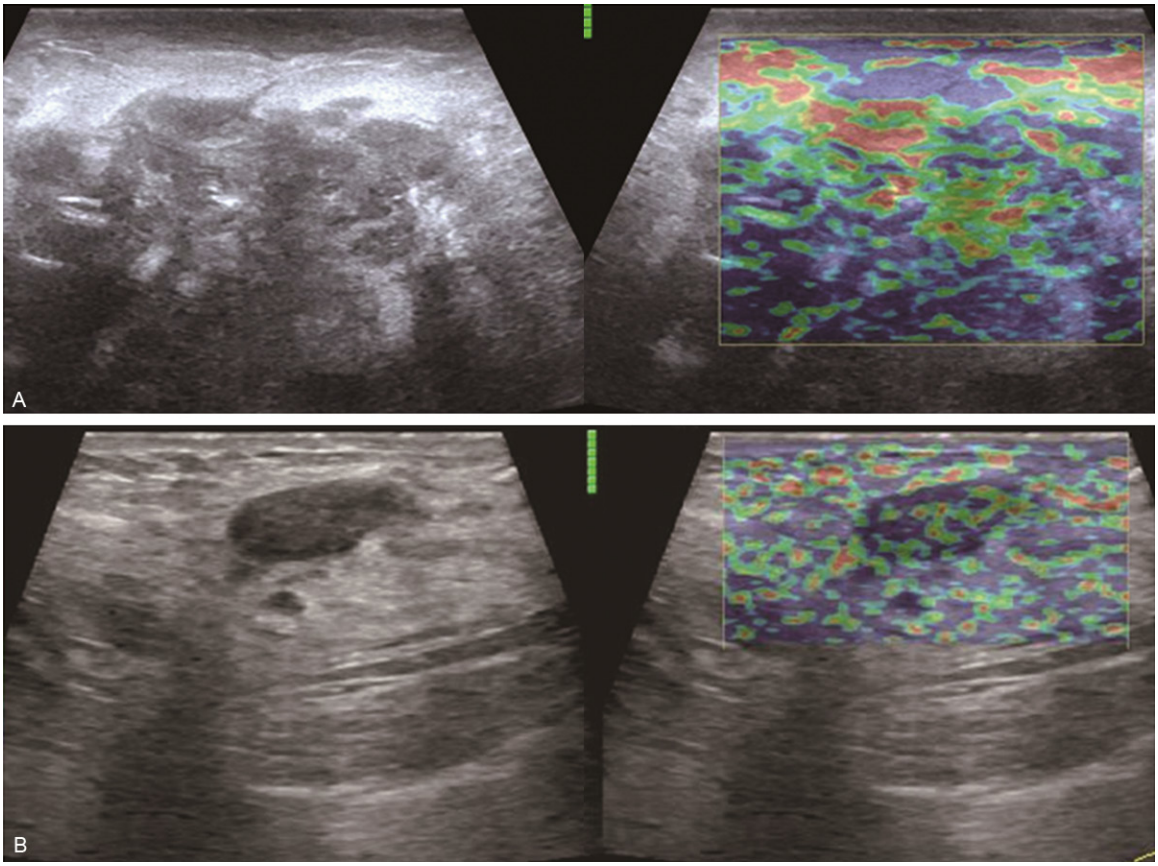

Figure 3. US of (A) a 39 year-old female with MDE complicated with inflammation, abscess, and granuloma when most lesions appeared green results indicating a score of 1; and (B) a 32 year-old female with MDE complicated with inflammation when most lesions appeared to be equally mixed green and blue, indicating a score of 3.

taking the medication. These data indicate that MDE can be diagnosed by US and MRI.

Discussion

Mammography and galactography are gradually being replaced by US and MRI examinations that have significantly higher resolution [6, 24, 25]. US examinations for mammary diseases include routine US and elastography. MRI examinations include plain MRI scans, diffusion-weighted imaging, dynamic contrast-enhancement scan, and ^{1}H MRS. Both US and MRI can provide quantitative or semi-quantitative information to improve diagnostic accuracy, including RI, elastography scores, ADC, EER, PER, Tpeak, time-intensity curve and tCho peak.

These techniques afford better diagnosis and differential diagnosis of breasts. For instance, Alhabshi et al. confirm that elastography increases the diagnostic specificity of conventional techniques for malignant breast lesions from 61.4 to 93% [12]. In addition, Suppiah et al. report that the sensitivity of DCE-MRI for the diagnosis of malignant breast tumor ranges between 94 and 100%, while the specificity

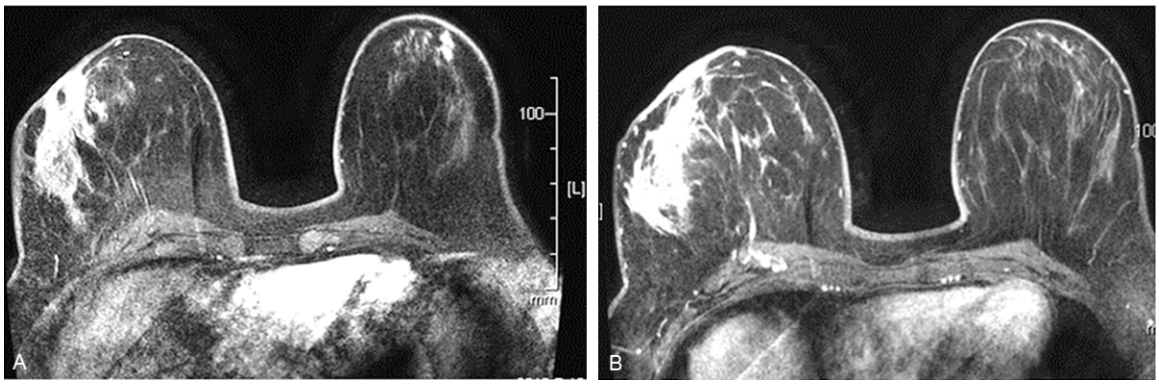

Figure 4. MRI plain-scan images of a 24 year-old female with MDE complicated with inflammation and granuloma obtained (A) before contrast medium injection and (B) after contrast medium injection. The lesion exhibits patchy and irregular enhancement, with clear boundaries, although the edge was not smooth.

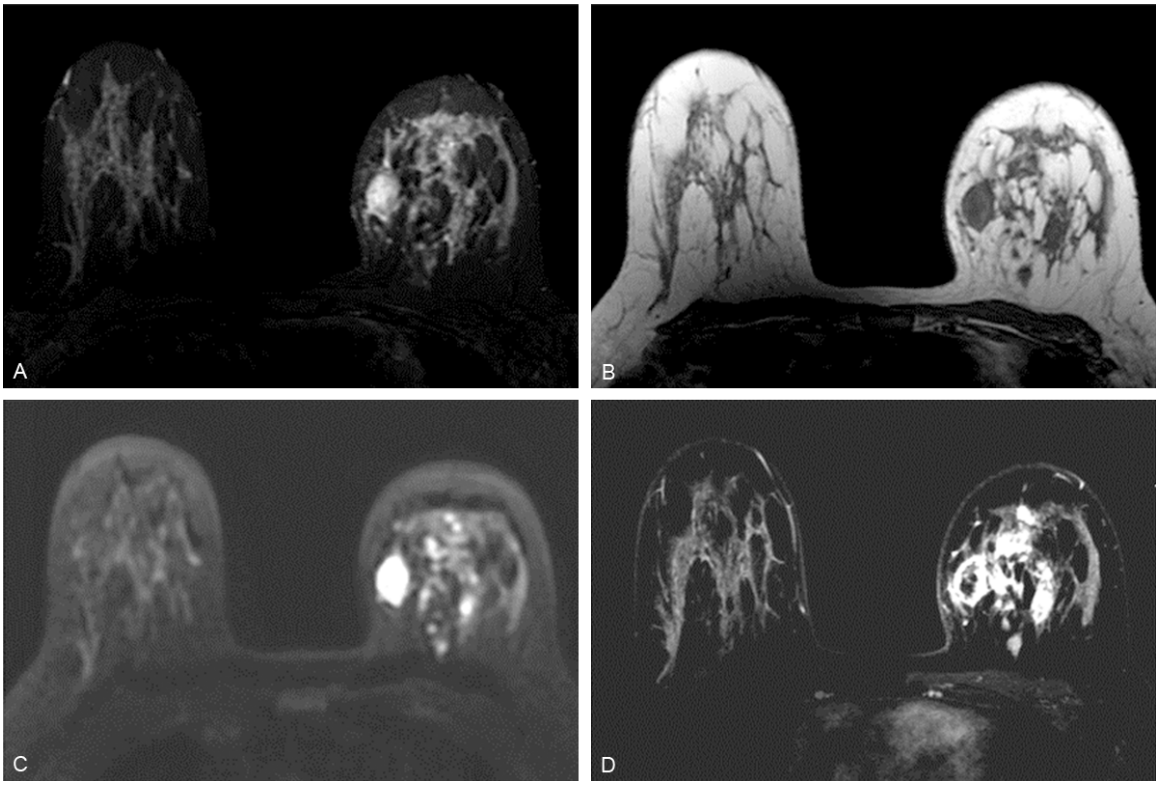

Figure 5. MRI plain-scan images of a 30 year-old female with MDE complicated. With inflammation and granuloma with (A) inhomogeneous high signal of STIR; (B) inhomogeneous low signal of T1FSE; (C) inhomogeneous high signal of diffusion-weighted imaging; and (D) heterogeneous ring-enhanced signal and enhanced signal of the mammary duct wall with a clear boundary.

ranges between 37 and 97%, which can be further increased from 70 to 92% with the assistance of MRS [15]. However, the ability of US and MRI to improve the sensitivity and specificity of MDE diagnosis has not been thoroughly investigated.

Though both mammography and US examinations are the primary tests for mammary diseases [9], squeezing of the mammary gland is usually required in mammography inspection, producing a potential risk of inflammatory diffusion for suspected MDE. Therefore, we did not

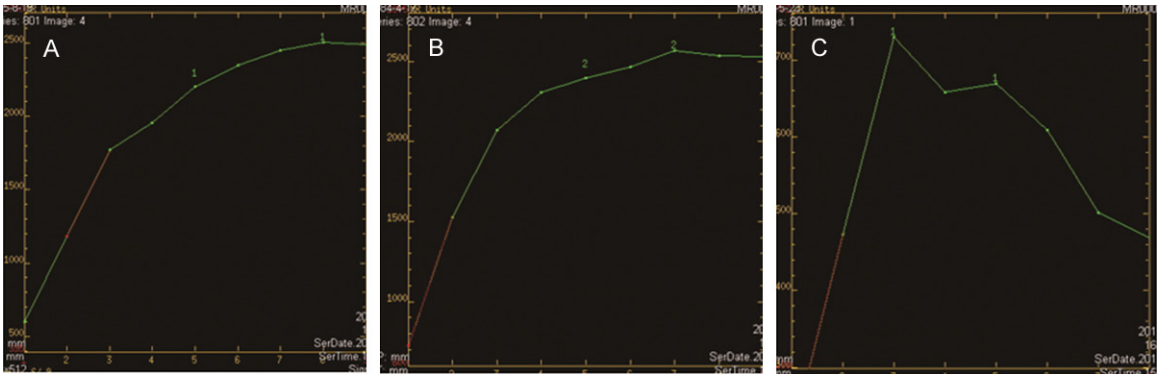

Figure 6. Three types of time-signal intensity curves. (A) Type I showing a persistently enhanced intensity of the dynamic signal. The intensity exceeded the cutoff point of 5%. (B) Type II showing a plateau in the middle and late stages after initial signal enhancement. The fluctuation of signal intensity ranged between ± 5%. (C) Type III showing declining signal intensity in the middle and late stages after initial signal enhancement. The decline exceeded the cutoff point of 5%.

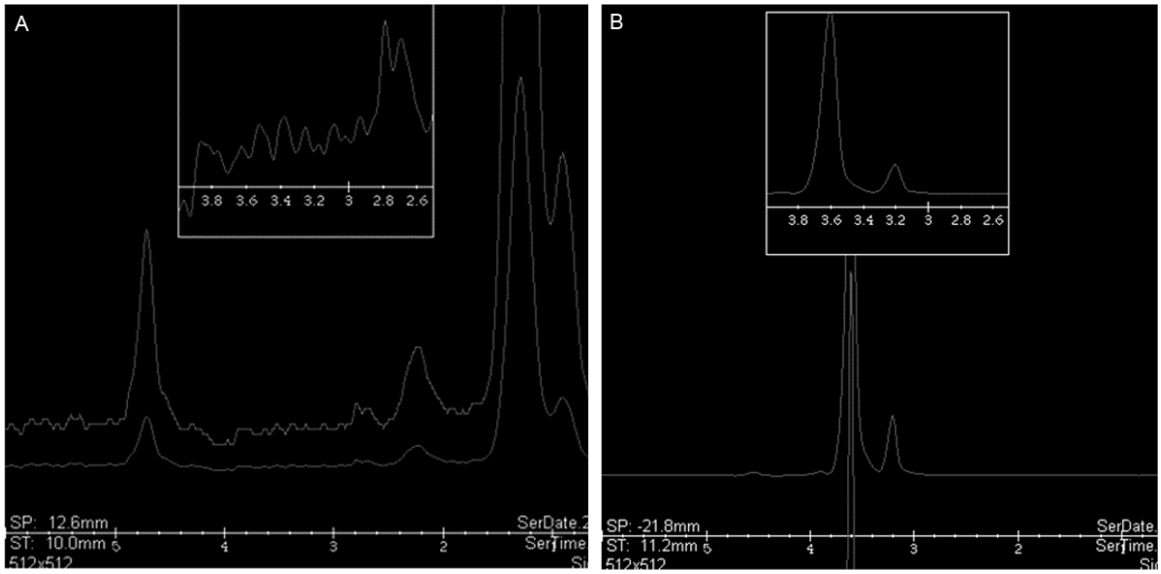

Figure 7. Magnetic resonance spectroscopy (MRS). (A) No MRS peak at 3.2 ppm for most MDE lesions. (B) MRS peak appeared at 3.2 ppm and 3.6 ppm for a 30-year-old female with MDE complicated with inflammation and granuloma misdiagnosed by MRI.

perform mammography examination in the present study. The present study showed that the average elastographic image value for MDE was 2.93 ± 0.77, which was lower than that of a malignant breast (4.2 ± 0.9) [13], indicating the significance of differential diagnosis between MDE and malignant breast. In this study, the RI of MDE was lower than 0.68, which was consistent with that reported by Jin and colleagues [26]. In addition, Hsu et al. found a significant predictive value of type III ultrasound images for malignant breast lesions [19]. In the present study, only 3 lesions out of 16 belonged to type III, indicating that the image type was informative for differentiating between benign and malignant lesions. Routine US, combined with elastography, can improve the specificity and accuracy of the diagnosis for breast tumors [27].

Magnetic resonance technology has become widely used in the diagnosis of mammary dis-

Table 4. Statistics

	US vs MRI	US vs combination	MRI vs combination	US vs MRI vs combination
x^2	0.762	3.2	7.467	2.139
P	0.450	0.25	0.125	0.467

Note: Differences are statistically significant if $P < 0.05$.

eases. Although plain magnetic resonance scan provides no specific findings related to MDE, T2-weighted imaging (T2WI) and diffusion-weighted imaging technologies clearly show the morphology, size and position of MDE lesions. In our study, the average ADC of MDE was 1.3 ± 0.19 mm^2/s, which was between those of benign and malignant lesions (1.5 ± 0.5 mm^2/s for benign and 1.2 ± 0.3 mm^2/s for malignant lesions) [28] and of no diagnostic significance for MDE. The commonly-used magnetic resonance parameters include EER, Tpeak and PER. The EER of DCE-MRI can reflect the vascular density in mammary glands and the clearance volume of contrast agent in lesions at early stages of scanning; Tpeak reflects the maximal aggregation of contrast agents in tumor tissue; and PER describes concentration changes of contrast agent from initial to peak. Malignant lesions typically have EER ≥ 80% (the value was obtained one minute after contrast agent injection), Tpeak of 219 s (ranging between 194 and 244), and PER of 1.44 (1.23 to 1.65) [29]. In this study, the average EER value was 67% (between 0.35 and 1.07) and 10 out of 16 lesions had values less than 80%; the average Tpeak was 248 s (ranging between 192 and 330); and the average PER was 2.59 (ranging between 2.26 and 3.06). All of these magnetic resonance parameters are higher than those for malignant lesions reported in published literatures, being indicators for the differentiation between MDE and malignant lesions. Studies indicate that TIC of type I MRI often occurs in benign lesions, type II indicates overlapped lesions that are both benign and malignant, and type III curves usually suggest malignant lesions [6]. In this study, 12 out of 16 lesions exhibited type I curve, which was consistent with published reports, implying the diagnostic significance of DCE-MRI for MDE. However, one lesion belonged to type III, leading to misdiagnosis. In addition, tCho peak occurred only in one lesion. As tCho peak usually appears in malignant lesions, this result suggests that benign lesions can also exhibit tCho peak.

Despite these interesting findings, the present study has some limitations. For example, the sample size was not large enough, lacking a control group with malignant lesions. Further study is required to confirm these findings. In summary, though there is no significant difference among the difference of diagnostic accuracies of US, MRI and the combination of US and MRI, this study demonstrates the potential clinical significance of US and MRI examinations for MDE diagnosis. Joint applications of UE, DCE-MRI and MRS imaging technologies can significantly improve MDE diagnosis accuracy.

Acknowledgements

This work was supported by the Shandong Provincial Science and Technology Development Program (No. 2014GSF118139).

Disclosure of conflict of interest

None.

Address correspondence to: Guangrui Shao, Department of Radiology, The Second Hospital of Shandong University, No. 247 Beiyuan Street, Jinan, Shandong Province, P.R. China. Tel: 86-15153169-055; Fax: 86-531-82666651; E-mail: sdshgr63@163.com

References

[1] Rahal RM, de Freitas-Júnior R, Carlos da Cunha L, Moreira MA, Rosa VD and Conde DM. Mammary duct ectasia: an overview. Breast J 2011; 17: 694-5.

[2] Duchesne N, Skolnik S and Bilmer S. Ultrasound appearance of chronic mammary duct ectasia. Can Assoc Radiol J 2005; 56: 297-300.

[3] Haagensen CD. Mammary-duct ectasia; a disease that may simulate carcinoma. Cancer 1951; 4: 749-61.

[4] Kim BS, Lee JH, Kim WJ, Kim DC, Shin S, Kwon HJ, Park JS and Park YM. Periductal mastitis mimicking breast cancer in a male breast. Clin Imaging 2013; 37: 574-6.

[5] Gioffrè Florio MA, Famà F, Buccheri G, Di Cara G, Pollicino A, Scarfò P and Gullo G. Non-lactational mastitis: our experience. Ann Ital Chir 2006; 77: 127-30.

[6] Ferris-James DM, Iuanow E, Mehta TS, Shaheen RM and Slanetz PJ. Imaging approaches to diagnosis and management of common ductal abnormalities. Radiographics 2012; 32: 1009-30.
[7] Ahmadinejad N, Movahedinia S, Movahedinia S and Shahriari M. Association of mammographic density with pathologic findings. Iran Red Crescent Med J 2013; 15: e16698.
[8] Tiu CM, Chiou SY, Chou YH, Lai CH, Chiou HJ, Chiang HR, Chen SP, Wang HK, Yen CS, Chang CY and Hsu CY. Clinical Significance of Ductal Dilatation on Breast Ultrasonogram. J Med Ultrasound 2005; 13: 127-134.
[9] Ferron S, Asad-Syed M, Boisserie-Lacroix M, Palussière J and Hurtevent G. Imaging benign inflammatory syndromes. Diagn Interv Imaging 2012; 93: 85-94.
[10] Kamal RM, Hamed ST and Salem DS. Classification of inflammatory breast disorders and step by step diagnosis. Breast J 2009; 15: 367-80.
[11] Renz DM, Baltzer PAT, Böttcher J, Thaher F, Gajda M, Camara O, Runnebaum IB and Kaiser WA. Magnetic resonance imaging of inflammatory breast carcinoma and acute mastitis. A comparative study. Eur Radiol 2008; 18: 2370-80.
[12] Alhabshi SMI, Rahmat K, Abdul Halim N, Aziz S, Radhika S, Gan GC, Vijayananthan A, Westerhout CJ, Mohd-Shah MN, Jaszle S, Harlina Mohd Latar N and Muhammad R. Semi-quantitative and qualitative assessment of breast ultrasound elastography in differentiating between malignant and benign lesions. Ultrasound Med Biol 2013; 39: 568-78.
[13] Bartolotta TV, Ienzi R, Cirino A, Genova C, Ienzi F, Pitarresi D, Safina E and Midiri M. Characterisation of indeterminate focal breast lesions on grey-scale ultrasound: role of ultrasound elastography. Radiol Med 2011; 116: 1027-38.
[14] Baltzer PAT, Dietzel M and Kaiser WA. MR-spectroscopy at 1.5 tesla and 3 tesla. Useful? A systematic review and meta-analysis. Eur J Radiol 2012; 81 Suppl 1: S6-9.
[15] Suppiah S, Rahmat K, Rozalli FI and Azlan CA. Re: Improved diagnostic accuracy in differentiating malignant and benign lesions using single-voxel proton MRS of the breast at 3 T MRI. A reply. Clin Radiol 2014; 69: e110-1.
[16] Alunni JP. Imaging inflammatory breast cancer. Diagn Interv Imaging 2012; 93: 95-103.
[17] Mansour SM and Abolfotooh A. Does MRI help in the assessment of inflammatory breast disorders? Egypt J Radiol Nucl Med 2012; 43: 487-497.
[18] Kok KY and Telisinghe PU. Granulomatous mastitis: presentation, treatment and outcome in 43 patients. Surgeon 2010; 8: 197-201.
[19] Hsu HH, Yu JC, Hsu GC, Chang WC, Yu CP, Tung HJ, Tzao C and Huang GS. Ultrasonographic alterations associated with the dilatation of mammary ducts: feature analysis and BI-RADS assessment. Eur Radiol 2010; 20: 293-302.
[20] Itoh A, Ueno E, Tohno E, Kamma H, Takahashi H, Shiina T, Yamakawa M and Matsumura T. Breast disease: clinical application of US elastography for diagnosis. Radiology 2006; 239: 341-50.
[21] Goddi A, Bonardi M and Alessi S. Breast elastography: A literature review. J Ultrasound 2012; 15: 192-8.
[22] Breast Imaging Reporting and Data System: (BI-RADS). 4th edition. Reston, VA: American College of Radiology; 2003.
[23] El Khouli RH, Macura KJ, Jacobs MA, Khalil TH, Kamel IR, Dwyer A and Bluemke DA. Dynamic contrast-enhanced MRI of the breast: quantitative method for kinetic curve type assessment. AJR Am J Roentgenol 2009; 193: W295-300.
[24] Campassi C, Cilotti A, Moretti M, Bagnolesi P, Liperi A De and Bartolozzi C. High-frequency ultrasound (10-13 MHz) in inflammatory diseases of the breast. Breast 1996; 5: 351-357.
[25] Le-Petross CH, Bidaut L and Yang WT. Evolving role of imaging modalities in inflammatory breast cancer. Semin Oncol 2008; 35: 51-63.
[26] Gong X, Wang Y and Xu P. Application of real-time ultrasound elastography for differential diagnosis of breast tumors. J Ultrasound Med 2013; 32: 2171-6.
[27] Jin G, Ding Z, Guo Y and Zhao X. Value of identifying and diagnosing mammary carcinoma and non-lactation mastitis lump by color Doppler ultrasonography. Chinese-German J Clin Oncol 2008; 7: 638-640.
[28] Hassan HH, Mahmoud Zahran MH, El-Prince Hassan H, Mohamed Abdel-Hamid AE and Abdel Shafy Fadaly G. Diffusion magnetic resonance imaging of breast lesions: Initial experience at Alexandria University. Alexandria J Med 2013; 49: 265-272.
[29] Kuhl CK, Mielcareck P, Klaschik S, Leutner C, Wardelmann E, Gieseke J and Schild HH. Dynamic breast MR imaging: are signal intensity time course data useful for differential diagnosis of enhancing lesions? Radiology 1999; 211: 101-10.